

Hohlraum-Driven High-Convergence Implosion Experiments with Multiple Beam Cones on the Omega Laser Facility

Peter Amendt, R. E. Turner, and O. L. Landen

Lawrence Livermore National Laboratory, Livermore, California 94550

(Received 21 March 2002; published 26 September 2002)

High-convergence implosion experiments have been performed on the Omega laser facility [T.R. Boehly *et al.*, *Opt. Commun.* **133**, 495 (1997)] using cylindrical gold hohlraums with 40 drive beams arranged into multiple cones. These experiments make use of improved hohlraum radiation symmetry conditions [T.J. Murphy *et al.*, *Phys. Rev. Lett.* **81**, 108 (1998)] to demonstrate near predicted primary (2.45 MeV) neutron production from single-shell implosions with measured deuterium fuel convergence ratios exceeding 20 at an ignition-relevant hohlraum case-to-capsule ratio ≈ 3 .

DOI: 10.1103/PhysRevLett.89.165001

PACS numbers: 52.57.-z, 52.50.Jm

The goal of inertial confinement fusion (ICF) is to implode a capsule filled with deuterium-tritium to a sufficient density and temperature for achieving thermonuclear ignition and energy gain [1]. In the indirect-drive option, a capsule is placed at the center of a hollow high-Z radiation enclosure or hohlraum which converts absorbed laser rays into x rays that ablate the outside of the fuel-filled capsule and drive an implosion. A necessary requirement for ignition of the fuel is that the x-ray flux symmetry have satisfactory uniformity to achieve a nearly symmetric implosion. The National Ignition Facility (NIF) [2] is planned to demonstrate ignition under hohlraum conditions where the rms time-integrated flux nonuniformities are $<2\%$ for the 16 ns duration of the laser drive [3]. A further requirement on the flux symmetry is that time-dependent asymmetry excursions not exceed 5%–10% over any 3 ns interval in the drive [3]. Given these symmetry constraints on the NIF, an experimental effort on the University of Rochester's Omega laser [4] is in place to diagnose and control hohlraum symmetry conditions as a prelude to the NIF. A stringent and integrated test of symmetry control on the Omega laser is the ability to achieve high-convergence implosions where convergence is defined as the initial capsule radius divided by the imploded fuel radius.

Time-integrated x-ray symmetry control has been demonstrated on the Omega laser [5] using a NIF-like multicone geometry (Fig. 1). Three cones consisting of 5, 5, and 10 beams enter each end of the gold hohlraum through a laser-entrance hole (LEH) at three distinct angles to the hohlraum symmetry axis: $\theta = 21.4^\circ$, 42° , and 58.9° . The energy of the $0.351 \mu\text{m}$ wavelength laser beams is absorbed by the gold hohlraum walls and is efficiently reradiated as a quasi-Planckian spectrum of x rays. Analysis and simulations show that high-spatial frequency x-ray drive variations are effectively smoothed as the radiation is transported from the hohlraum wall to the capsule surface. The degree of flux symmetrization improves as the case-to-capsule ratio is increased, but at

the expense of reduced energy absorbed by the capsule. The baseline NIF target design uses a hohlraum case-to-capsule ratio of ≈ 2.5 and delivers 150 kJ of energy to the capsule compared to 1.8 MJ of available laser energy [3]. For such a moderate case-to-capsule ratio low spatial-frequency drive variations are not effectively smoothed by radiation transport alone, and alternative methods must be implemented. The symmetry-control techniques envisioned for the NIF include (1) using multiple beam cones per side, (2) using hohlraum gasfills to limit the spatial excursions of the laser absorption regions or "hot spots," (3) changing the relative power (via "beam phasing") between the inner and outer laser cones for dynamic symmetry control and added ignition margin, and (4) using high-Z mixtures in the hohlraum wall for reducing the x-ray emissivity contrast between the unirradiated wall and the laser hot spots [6].

The hohlraum symmetry effort on Omega has focused to date on approaching the required symmetry criteria for a NIF-like case-to-capsule ratio by exploiting the first technique, i.e., use of the multicone geometry [5,7,8]. Recent studies have confirmed a large improvement in capsule performance on Omega for moderate convergence (≈ 9) indirectly driven capsules [9] compared to its 10 beam, single-cone predecessor, the

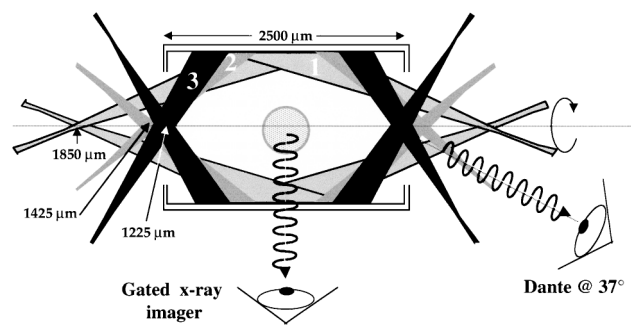


FIG. 1. Schematic of hohlraum geometry and Omega laser cone configurations with indicated diagnostic lines of sight and beam pointings relative to the hohlraum center.

Nova laser [10]. A useful figure of merit for implosion performance is the ratio of the measured primary $\{D + D \rightarrow n(2.45 \text{ MeV}) + \text{He}^3(0.82 \text{ MeV})\}$ neutron yield to the simulated one-dimensional (1D) “clean” neutron yield, or so-called “yield over clean” ($\text{YoC}_{1\text{D}}$). A clean yield refers to the calculated neutron yield excluding the performance degrading effects of hydrodynamic instability. On Nova the $\text{YoC}_{1\text{D}}$ for moderate convergence implosions was typically about 25% [11], whereas on Omega the $\text{YoC}_{1\text{D}}$ is about 3 times larger [9]. The four reasons for this reported improvement are ascribed to (1) the factor-of-3 reduction in time-dependent lowest-order (2nd Legendre) flux asymmetry swings inherent to the multicone geometry [9], (2) the reduced time-integrated 4th Legendre distortion also inherent to the multicone geometry [9], (3) the greater azimuthal flux symmetry arising from having on average $2\times$ more beams/cone, and (4) the $2\times$ reduction in random flux asymmetries due to having $4\times$ more beams with similar beam-to-beam power balance.

In this Letter we exploit the improved hohlraum symmetry conditions on Omega to demonstrate high-convergence implosions for a NIF-relevant case-to-capsule ratio of ≈ 3 . The reported high convergences (≈ 20) are inferred from secondary $\{D + T(<1.01 \text{ MeV}) \rightarrow n(11.8\text{--}17.1 \text{ MeV}) + \text{He}^4\}$ neutron measurements with the Medusa detector [12] which provide a sensitive indicator of the compressed fuel areal density [13]. This result represents a factor-of-2 improvement in the highest observed convergence to date of an indirectly driven single-shell capsule for a NIF-like case-to-capsule ratio. Similar high convergences have been reported previously with indirect drive but either under conditions of large case-to-capsule ratio (> 6) for flux asymmetry mitigation on Nova [14] and Omega [15] or in double-shell experiments on Omega where the fuel convergence is generously defined relative to the *outer* shell radius [16].

Figure 1 shows the Omega hohlraum geometry used for our high-convergence implosion studies. The “scale-1” thin wall gold hohlraums were $2500 \mu\text{m}$ long with a radius of $800 \mu\text{m}$ and $600 \mu\text{m}$ radii LEHs. The hohlraum wall consisted of $2 \mu\text{m}$ of Au overcoated with $50 \mu\text{m}$ of epoxy to accommodate noninvasive x-ray imaging of the fuel-pusher region at peak x-ray emission. The 40 laser beams with nominally identical power history were positioned along the hohlraum symmetry axis to give the best time-integrated lowest-order flux symmetry at the capsule. The capsule was a CH (plastic) shell of nominal $30 \mu\text{m}$ thickness and inner radius of $220 \mu\text{m}$. The shell is doped with 1% Ge to mitigate volumetric x-ray preheat above the $n = 2$ bound-free absorption edge of Ge (1.2 keV). Deuterium (D_2) is used as the fuel fill and the convergences are varied by adjusting the room temperature fuel pressure between 5 and 50 atm.

Figure 2 shows the laser power history used to drive the hohlraums. The nominal energy of 14 kJ is equally distributed within 2.5 ns over 40 beams and uses a two-step

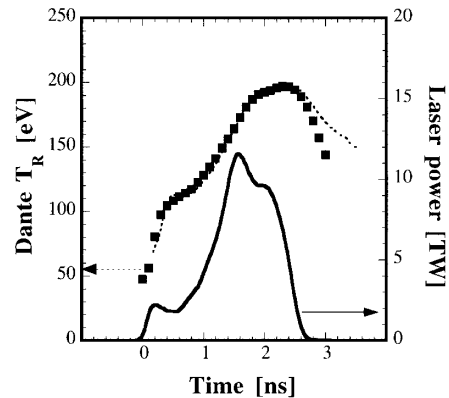


FIG. 2. Measured (filled squares) and simulated (dashed line) Dante drive temperature versus time; total laser power history (solid line) versus time.

pulse shape for efficient compression of the fuel. Also shown is the measured and calculated x-ray drive history as seen by Dante [17], an array of x-ray diodes positioned at 37° to the hohlraum axis outside the LEH (see Fig. 1). The calculations are based on integrated hohlraum radiation-hydrodynamics simulations [18] and postprocessed to simulate the Dante view of the hohlraum wall and laser hot spots through the LEH [19]. The agreement between the measured and calculated drive temperature is very close and suggests weak levels of backscatter losses which have not been included in the simulations. Indeed, full-aperture backscatter (FABS) measurements on (outer) cones 2 and 3 show total backscatter levels into the $f/6$ lens cones generally less than 100 J/cone; near backscatter outside of the monitoring lenses is estimated to be at a similar level based on near backscatter imaging experience on Nova [20]. Cone 1 FABS monitoring is not yet available on Omega but comparison of the length of hohlraum plasma traversed and wall intensity with the geometry of cone 2 argues for a total cone 1 backscatter level of $\approx 200 \text{ J}$. Thus, we infer a total backscatter level of only $\approx 600 \text{ J}$ or 4% of the incident laser energy, corresponding to an imperceptible $\approx 3 \text{ eV}$ deficit in peak drive temperature.

Measured peak x-ray emission times from the imploded core provide a further check on the hohlraum drive. Figure 3 shows a comparison of the measured and simulated peak x-ray emission times for the three capsule types. The good agreement verifies that the hohlraum drive is properly modeled in the calculations which is critical for reliably simulating implosion performance.

The traditional figure of merit for modeling ICF implosion performance is the ratio of observed primary (DD) neutron yield to the simulated DD neutron yield. Figure 4(a) shows the measured DD neutron yields, normalized to calculated clean DD neutron yields from two-dimensional (2D) integrated hohlraum simulations [21], versus the measured fuel convergence. The convergence is inferred from the ratio of secondary (DT) neutron yield, as recorded by a time-resolved neutron sensitive

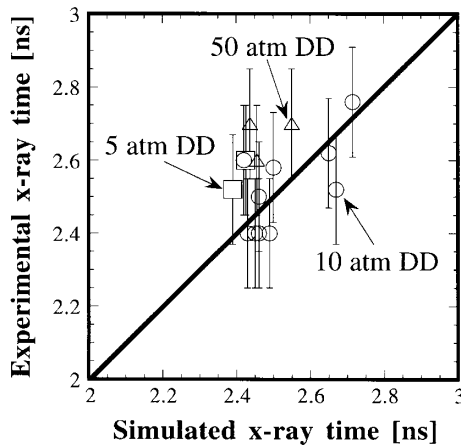


FIG. 3. Measured versus simulated instant of peak x-ray self-emission for 5 atm D_2 -filled capsules (open squares), 10 atm D_2 -filled capsules (open circles), and 50 atm D_2 -filled capsules (open triangles).

scintillator array — Medusa [12], to the DD neutron yield. Specifically, the measured DT/DD neutron ratio determines the fuel areal density $\langle \rho R \rangle$ and, hence, by conservation of fuel mass, the convergence through use of a “hot spot” model [13] and accounting for triton slowing in a plasma with ≈ 1 keV ion temperature. The hot spot model assumes that all primary reaction products are created at the center of a spherical fuel volume with uniform (ion) temperature and density. Figure 4(a) shows that the highest convergence targets at 5 atm D_2 fill had a mean YoC_{2D} performance near 30%, including the effects of intrinsic hohlraum (2D) flux asymmetry. As indicated by the YoC_{1D} values in Fig. 4(a) the degradation due to hohlraum asymmetry alone can still lead to a factor-of-3 degradation at the highest reported convergence.

To explain the residual degradation in performance indicated in Fig. 4(a) we have used a Haan-type mix analysis [22] to assess the role of the Rayleigh-Taylor instability at the fuel-pusher interface. Calculations suggest that perturbations on this interface are primarily seeded by feedthrough of outer surface perturbations during shock transit. Each target was measured for outer surface roughness, and the resulting power spectrum was convolved with a calculated linear growth factor spectrum to generate a time-dependent mode spectrum on the inner surface of the shell. For each type of capsule we calculated the linear growth factor spectrum and found peak values, defined as the final-to-initial amplitude, in excess of 200. The 5 and 10 atm D_2 -filled capsules both attain maximum growth near $l_{max} \approx 20$, while for the low convergence capsule, $l_{max} \approx 30$, where l is the Legendre mode number of the surface perturbation. For comparison, the expected growth factor on the NIF is 400–1000 [1]. The Haan prescription for weakly non-linear saturation is applied and the resulting spectrum of modes is summed in quadrature to generate a time-varying mix region. The yield degradation in a 1D simulation with a dynamic mix layer is then multiplicatively

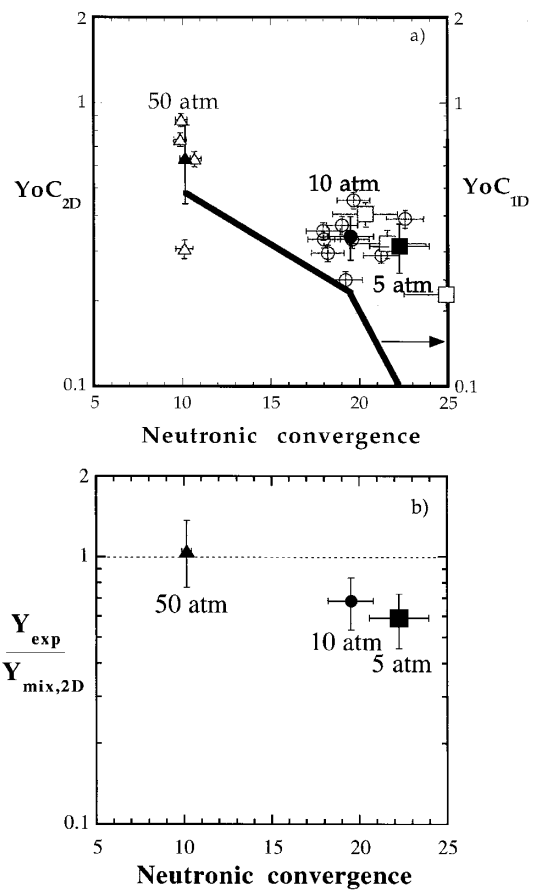


FIG. 4. (a) Ratio of measured primary (DD) neutron yield-over-clean 2D simulated yield YoC_{2D} versus inferred fuel convergence from secondary (DT) neutrons for 5 atm D_2 -filled capsules (open squares), 10 atm D_2 -filled capsules (open circles), and 50 atm D_2 -filled capsules (open triangles). Solid symbols denote averaging over each target type; solid line indicates corresponding averaged measured yield-over-clean 1D (symmetrized 2D) simulated yields (YoC_{1D}). (b) Averaged ratio of measured primary (DD) neutron yield to 2D simulated yield with 1D mix model versus inferred fuel convergence from secondary (DT) neutrons.

applied to a clean 2D integrated hohlraum simulation prediction to estimate the combined effect of mix and intrinsic radiation asymmetry on DD neutron performance. Figure 4(b) shows the result of this procedure applied to the three types of capsule. The performance of the lowest convergence targets matches well the predicted DD neutron yields according to our prescription for degradation from mix and flux asymmetry. Other sources of degradation such as long-wavelength ($l = 2$) capsule nonuniformities and random flux asymmetry from laser power imbalances exist but are estimated to contribute less than 10% in total. Thus, for the higher convergence targets, Fig. 4(b) shows that a 20%–30% yield degradation still remains. However, most of this degradation can be explained by the effects of a plausible $0.5 \mu\text{m}$, $l = 1$ shell thickness variation which alone can contribute a 20% degradation in yield [23].

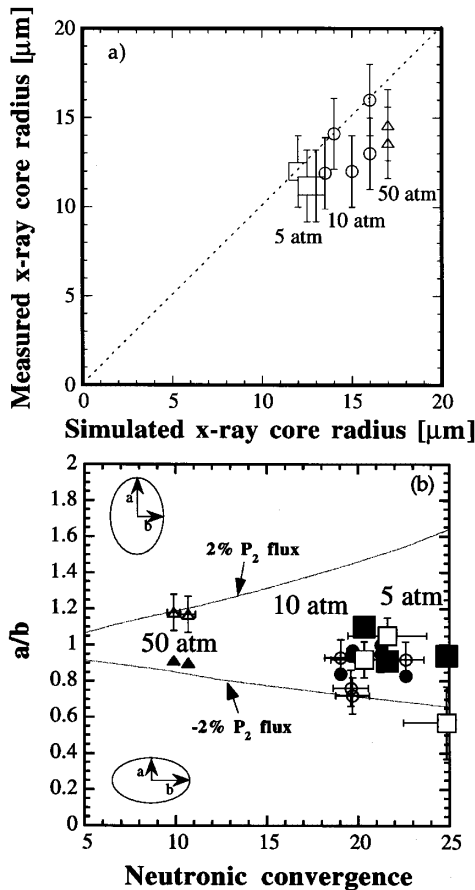


FIG. 5. (a) Measured versus 2D simulated average radius of 50% x-ray self-emission contour. (b) Measured (open symbols) and simulated (solid symbols) “ a/b ” distortion of 50% x-ray self-emission contour versus inferred fuel convergence for 5 atm D₂-filled capsules (squares), 10 atm D₂-filled capsules (circles), and 50 atm D₂-filled capsules (triangles); contours show predicted a/b distortion from imposed $\pm 2\%$ P_2/P_0 flux asymmetry.

Multiple 4–6 keV x-ray images of the imploded cores were obtained using an array of 5 μm pinholes and 70 ps resolution framing cameras. Figure 5(a) shows the comparison between the measured and expected 50% self-emission contour sizes for fuel bremsstrahlung x rays. This contour correlates well with the fuel-pusher interface for the higher convergence capsules, i.e., 5 and 10 atm D₂ fill, according to the simulations. For the lowest convergence capsules, i.e., 50 atm D₂ fill, the core (electron) conditions are ($\approx 2.5\times$) less isothermal, giving more localized emission at the core and a less reliable indicator of fuel size based on a 50% x-ray self-emission contour. A lower intensity contour could be chosen to better match the location of the fuel-pusher interface, but such an exercise is intrinsically model dependent and illustrates the disadvantage of inferring a fuel convergence from x-ray core imaging alone [16,24]. Figure 5(b) shows the measured distortions of the 50% emission contour versus inferred convergence from secondary neutron measure-

ments. The standard metric for core distortion is “ a/b ,” where a (b) is the radius of the 50% contour along the hohlraum waist (axis). The two contours correspond to a predicted core distortion from an assumed NIF-relevant rms time-integrated lowest-order flux asymmetry of $\pm 2\%$. Overall, the data show effective symmetry control at the highest convergences near the level of flux uniformity required for the NIF.

In summary, we have demonstrated repeatable, near-calculated performance of hohlraum-driven high-convergence (≈ 20) single-shell implosions with the Omega laser using a NIF-like hohlraum geometry. The demonstrated laser power balance and radiation uniformity have satisfactorily reduced the sources of random and intrinsic ($l = 2, 4$) flux asymmetry to levels required for demonstrating ignition on the NIF. Demonstration of even higher ignition-relevant convergences (> 30) via secondary neutron measurements is not considered possible with the Omega laser due to the energy limitation (≈ 20 kJ) and must await the much higher energy projected for the NIF.

We acknowledge useful discussions with Mike Campbell, Steve Haan, Bruce Hammel, John Lindl, and Larry Suter. We are indebted to Russ Wallace for target fabrication and to the Omega team for operational support. This work was performed under the auspices of the U.S. Department of Energy by the Lawrence Livermore National Laboratory under Contract No. W-7405-Eng-48.

- [1] J. D. Lindl, *Inertial Confinement Fusion* (Springer-Verlag, New York, 1998).
- [2] J. A. Paisner *et al.*, *Laser Focus World* **30**, 75 (1994).
- [3] S. W. Haan *et al.*, *Phys. Plasmas* **2**, 2480 (1995).
- [4] T. R. Boehly *et al.*, *Opt. Commun.* **133**, 495 (1997).
- [5] T. J. Murphy *et al.*, *Phys. Rev. Lett.* **81**, 108 (1998).
- [6] L. J. Suter *et al.*, *Phys. Plasmas* **7**, 2092 (2000).
- [7] O. L. Landen *et al.*, *Phys. Plasmas* **6**, 2137 (1999).
- [8] R. E. Turner *et al.*, *Phys. Plasmas* **7**, 333 (2000).
- [9] R. E. Turner *et al.* (to be published).
- [10] E. M. Campbell, *Laser Part. Beams* **9**, 209 (1991).
- [11] M. M. Marinak *et al.*, *Phys. Plasmas* **3**, 2070 (1996).
- [12] J. P. Knauer *et al.*, *Rev. Sci. Instrum.* **66**, 926 (1995).
- [13] H. Azechi, M. D. Cable, and R. O. Stapf, *Laser Part. Beams* **9**, 119 (1991).
- [14] M. D. Cable *et al.*, *Phys. Rev. Lett.* **73**, 2316 (1994).
- [15] G. R. Bennett *et al.*, *Phys. Plasmas* **7**, 2594 (2000).
- [16] W. S. Varnum *et al.*, *Phys. Rev. Lett.* **84**, 5153 (2000).
- [17] H. N. Kornblum, R. L. Kauffman, and J. A. Smith, *Rev. Sci. Instrum.* **57**, 2179 (1986).
- [18] G. B. Zimmerman and W. L. Kruer, *Comments Plasma Phys. Control. Fusion* **2**, 51 (1975).
- [19] C. Decker *et al.*, *Phys. Rev. Lett.* **79**, 1491 (1997).
- [20] R. K. Kirkwood *et al.*, *Rev. Sci. Instrum.* **68**, 636 (1997).
- [21] L. J. Suter *et al.*, *Phys. Rev. Lett.* **73**, 2328 (1994).
- [22] S. W. Haan, *Phys. Rev. A* **39**, 5812 (1989).
- [23] J. D. Lindl *et al.* (to be published).
- [24] J. M. Wallace *et al.*, *Phys. Rev. Lett.* **82**, 3807 (1999).